Inorganic Chemistry

Article

pubs.acs.org/IC

Gold(I)-Coordination Triggered Multistep and Multiple Photochromic Reactions in Multi-Dithienylethene (DTE) Systems

Bin Li,[†] Yu-Hui Wu,[†] Hui-Min Wen,[†] Lin-Xi Shi,[†] and Zhong-Ning Chen*[,†,‡]

[†]State Key Laboratory of Structural Chemistry, Fujian Institute of Research on the Structure of Matter, Chinese Academy of Sciences, Fuzhou, Fujian 350002, China

[‡]State Key Laboratory of Organometallic Chemistry, Shanghai Institute of Organic Chemistry, Chinese Academy of Sciences, Shanghai 200032, China

Supporting Information

ABSTRACT: The preparation, characterization, and photochromic properties of a mononuclear gold(I) complex (**1oo**) with two identical DTE-acetylides and a dinuclear gold(I) complex (**2ooo**) with both DTE-acetylide and DTE-diphosphine are described. Both gold(I) complexes exhibit multistep and multiple photocyclization/cycloreversion reactions. Particularly, four-state and four-color photochromic switch is successfully achieved for the dinuclear gold(I) complex upon irradiation with appropriate wavelengths of light. In contrast, fully ring-closed form is unattained through multiple photocyclization for the two corresponding model organic compounds coupling with the same DTE units as gold(I) complexes but without gold(I)-participation. It is demonstrated that coordination of gold(I) ion to DTE-acetylides exerts indeed a crucial role in achieving stepwise and selective photocyclization and cycloreversion reactions for both gold(I) complexes, in which the coordinated gold(I) atom acts as an effective "barrier" to prohibit intramolecular energy transfer between multi-DTE moieties.

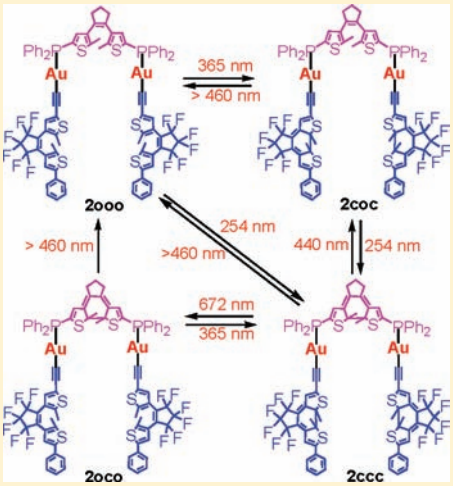

INTRODUCTION

Photochromic dithienylethene (DTE) compounds that can undergo reversible color changes through photochemical reactions have been found to exhibit extensive applications in optical memory, optoelectronics, and switching devices at molecular level.[1−3] Photochromic switches that can afford multicolors and multistates upon irradiation with appropriate wavelengths of light are particularly significant for achieving multifrequency optical memories and data storages.[4,5] Nevertheless, multistep and multiple photochromic reactions in a combined molecule with multidithienylethene (DTE) units are usually inaccessible because of facile intercomponent energy transfer from ring-open DTE to adjacent ring-closed moiety that prohibits further photocyclization to attain fully ring-closed form.[2,3] Although a few organic compounds containing multi-DTE units have been reported to exhibit distinctly selective and multicolor photochromic properties,[4a,b,d] the fully ring-closed isomers are always unattainable. To our knowledge, only a platinum(II)-coordinated complex with two identical DTE units has been recently described to display stepwise and dual photochromic reactions.[6] Thus, it is highly challenging to achieve multistep and multiple photochromic reactions.

On the other hand, incorporation of photoresponsive molecules into metal-coordinated systems is one of the feasible approaches to modulate the photochromic properties by simply changing the nature of the metal-coordinated component without modifying the photochromic moiety.[7−29] Although multistep and multiple photocyclization reactions to attain fully ring-closed form are mostly unattainable in the reported metal complexes with multi-DTE units,[7,8,22−28] we believe that by elaborate design and judicious choice of the ligands and the metal centers, incorporating multi-DTE moieties into a proper metal-coordinated system may overcome intramolecular energy transfer, thus providing a possible approach to achieve multistep and multiple photochromic reactions in a multi-DTE metal complex.

Considering that gold(I) ion may serve as such an effective "barrier" to prohibit rapid intercomponent energy transfer between the coordinated DTE moieties, we designed and prepared a mononuclear gold(I) complex **1oo** (Scheme 1) containing two DTE-acetylides as well as a dinuclear gold(I) complex **2ooo** (Scheme 2) that incorporates one DTE-diphosphine (L1o)[29] and two DTE-acetylide (L2o)[21] ligands. As expected, stepwise and multiple photocyclization/cycloreversion reactions are indeed achieved for both **1oo** and **2ooo**. More importantly, four-state and four-color photochromic switch is successfully achieved for **2ooo** upon irradiation with appropriate wavelengths of light. In contrast, fully ring-closed form is unattained through multiple photocyclization for the

Received: October 19, 2011
Published: January 18, 2012

   dx.doi.org/10.1021/ic202265u | *Inorg. Chem.* 2012, 51, 1933−1942

Scheme 1. Synthetic Routes for Gold(I) Complex 1oo and the Corresponding Model Compound 3oo

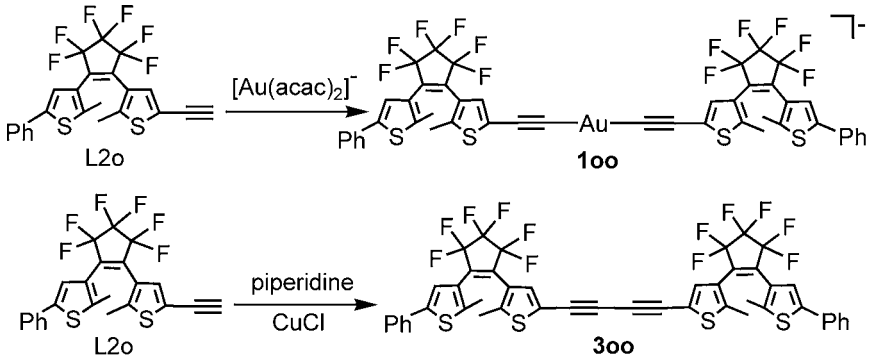

Scheme 2. Synthetic Routes for Dinuclear Gold(I) Complex 2ooo and the Corresponding Model Compound 4ooo

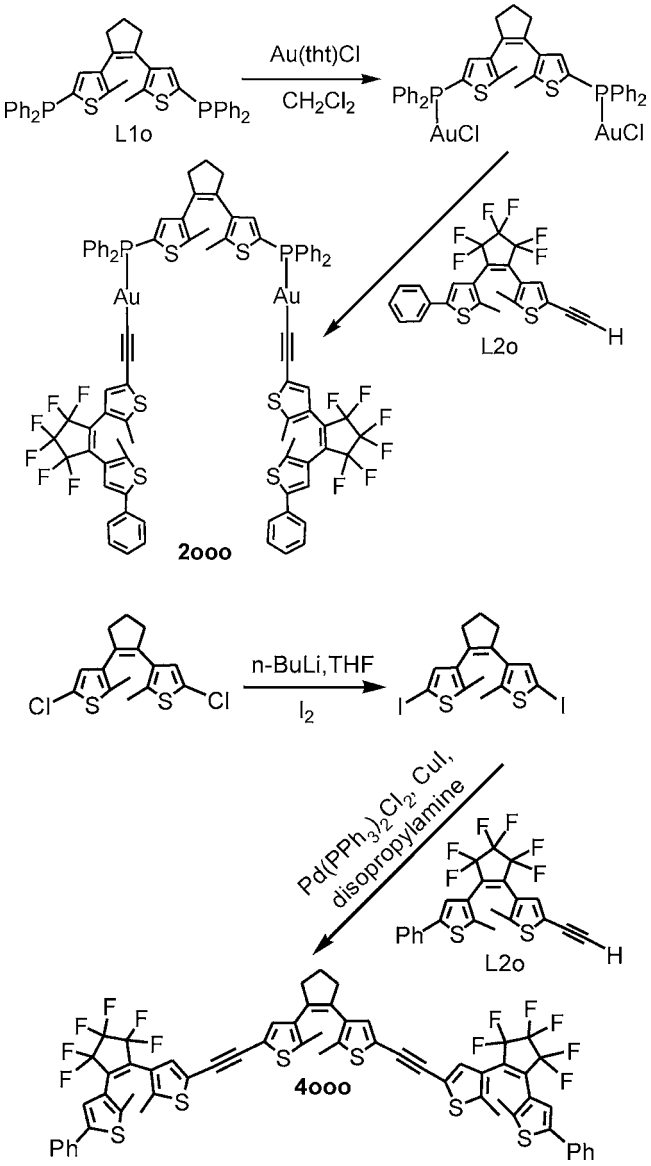

corresponding model organic compound **3oo** (Scheme 1) or **4ooo** (Scheme 2) coupling with the same DTE units as gold(I) complex **1oo** or **2ooo** but without gold(I)-participation. Thus, gold(I) coordination to DTE-acetylides exerts indeed a crucial role in achieving stepwise and multiple photocyclization/cycloreversion reactions for both **1oo** and **2ooo**.

RESULTS AND DISCUSSION

Complex **1oo** was prepared by the reaction of $[Au(acac)_2]^-$ with 2 equiv DTE-ethynyl ligand (L2o) in acetone (Scheme 1). Complex **2ooo** with mixed DTE-diphosphine (L1o) and DTE-ethynyl (L2o) ligands was synthesized by a two-step approach (Scheme 2). Diphosphine ligand L1o reacted first with 2 equiv Au(tht)Cl to give diphosphine-linked dinuclear gold(I) complex $Au_2(L1o)Cl_2$. The reaction of $Au_2(L1o)Cl_2$ with 2.2 equiv alkynyl ligand L2o in THF-MeOH solution afforded the desired product **2ooo** in 48% yield. The corresponding model organic compound **3oo** (Scheme 1) or **4ooo** (Scheme 2) with the same DTE units as gold(I) complex **1oo** or **2ooo** was prepared through carbon−carbon coupling reaction in high yield.

When colorless L1o or L2o in CH_2Cl_2 solution is irradiated under UV light at 254 or 365 nm, the color turns into red or blue, respectively. Meanwhile a broad absorption band centered at 510 or 584 nm (Figure S1) is observed for ring-closed isomer L1c or L2c, respectively. The conversion percentage is 53% for L1 and >95% for L2 at the photostationary state (PSS).

Stepwise and Dual Photochromism for 1oo. Upon irradiation of gold(I) complex **1oo** at 365 nm (Figure 1a), while the intense absorptions at 276 and 306 nm are gradually decreased, three new bands centered at 341, 386, and 608−622 nm are progressively increased due to the ongoing photocyclization reaction of L2o to L2c. Some progressive red-shift (Figure 1a) of the asymmetric visible absorption band with the maximum from 608 to 622 nm is most likely ascribed to stepwise photocyclization reactions **1oo**→**1co**→**1cc** (Scheme 3). In contrast, when model compound **3oo** is irradiated at 365 nm (Figure 1b) to the PSS, the new visible absorption band centered at 620 nm is symmetric with the absorbance being much lower (ca. 50% of **1**) than that for complex **1**, implying that **3oo** is simply converted to **3co**, whereas dually ring-closed form **3cc** is obviously not generated (Scheme 3).

When **1oo** in CD_2Cl_2 is irradiated with UV light at 365 nm, the ^1H NMR spectral signals (Figure 2a) at 7.25 ppm for H_{1o} and 6.94 ppm for H_{2o} are gradually weakened, whereas two new signals at 6.62 ppm for H_{1c} and 6.15 ppm for H_{2c} are increasingly enhanced. Upon sufficient irradiation at 365 nm, the signals at 7.25 ppm for H_{1o} and 6.94 ppm for H_{2o} vanished entirely, implying a full conversion of **1oo** to **1cc** through intermediate state **1co**. As depicted in Scheme 3 and Figure 2a, the CH_3 protons of **1oo** are observed at 1.92 (methyl *a*) and 1.81 ppm (methyl *b*). Upon irradiation of **1oo** at 365 nm, the

dx.doi.org/10.1021/ic202265u | Inorg. Chem. 2012, 51, 1933−1942

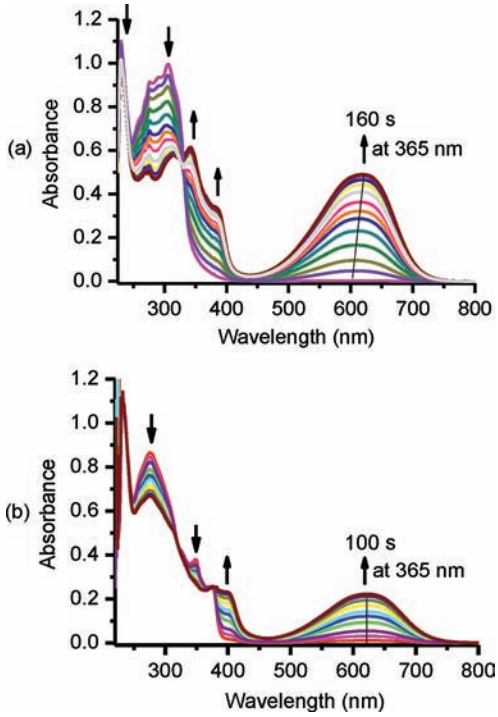

Figure 1. UV−vis absorption spectral changes of **1oo** (a) and **3oo** (b) in CH_2Cl_2 at 298 K upon irradiation at 365 nm.

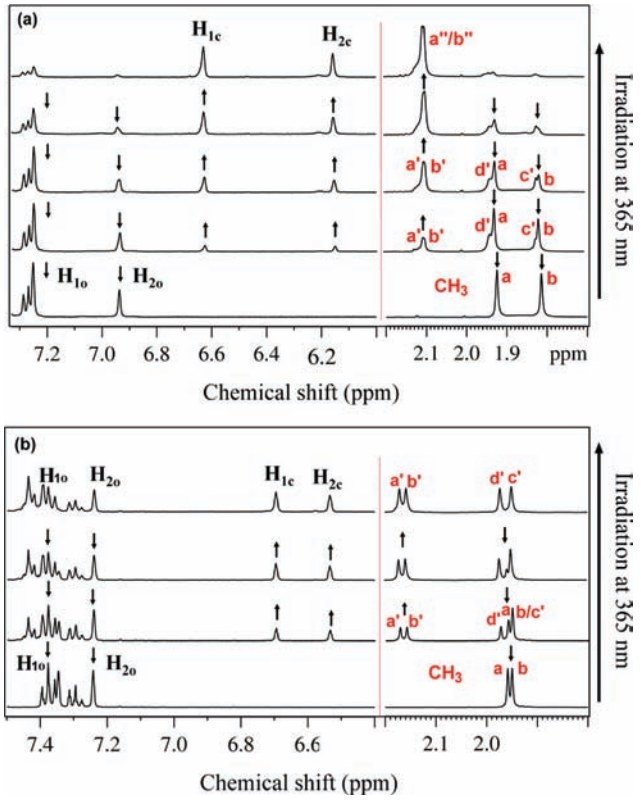

Figure 2. ^{1}H NMR spectral changes of **1oo** (a) and **3oo** (b) in CD_2Cl_2 upon irradiation at 365 nm to the PSS, showing (a) **1oo**→**1co**→**1cc**, and (b) **3oo**→**3co** conversions. The proton numbering is shown in Scheme 3.

two methyl signals are gradually attenuated with the occurrence of a new methyl signal at 2.10 ppm (methyl *a*′ and methyl *b*′) and two new methyl signals at 1.94 (methyl *d*′) and 1.83 (methyl *c*′) ppm with slight low-field shift relative to methyl signals *a* (1.92 ppm) and *b* (1.81), suggesting occurrence of **1oo**→**1co** conversion due to the photocyclization reaction of one of the two DTE moieties. Further keeping irradiation at 365 nm results in gradual decrease in intensity and finally entire disappearance for both methyl signals of **1oo** (signals *a* and *b*) and **1co** (signals *c*′ and *d*′), whereas overlapping methyl signals *a*″ and *b*″ at 2.10 ppm are only observed because of further photocyclization reaction of the other DTE to produce dual photocyclization form **1cc**. Thus, the variations of methyl proton signals demonstrate unambiguously that stepwise photocyclization reactions **1oo**→**1co**→**1cc** are indeed operating.

In contrast, when model compound **3oo** in CD_2Cl_2 is irradiated at 365 nm to the PSS, the ^{1}H NMR spectral signals (Figure 2b) at 7.37 ppm for H_{1o} and 7.24 ppm for H_{2o} do not

Scheme 3. Photochromic Reactions for 1oo and 3oo

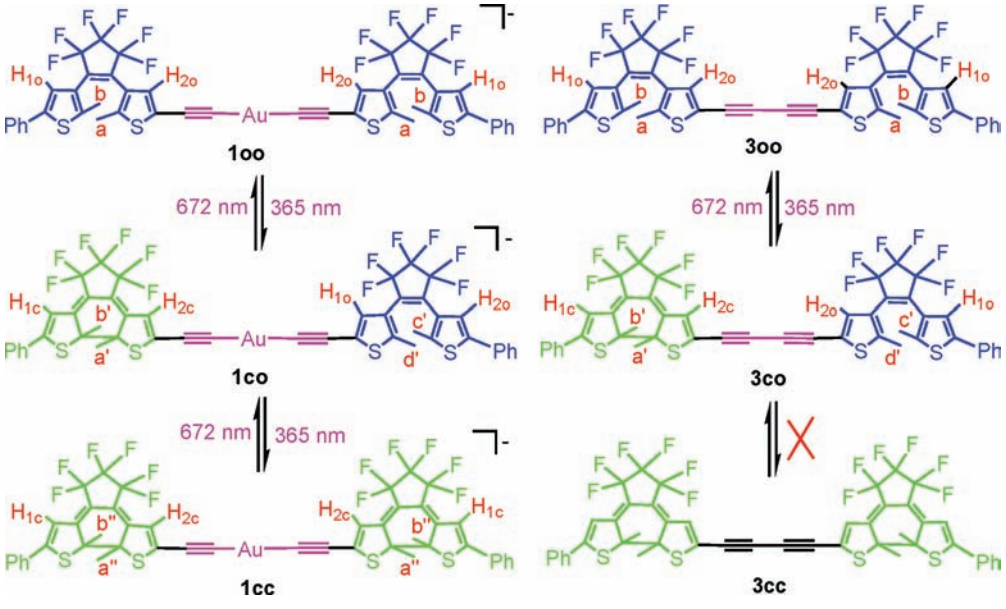

dx.doi.org/10.1021/ic202265u | *Inorg. Chem.* 2012, 51, 1933−1942

vanish entirely, and in fact their integral areas are almost the same as those of the new signals at 6.70 ppm for H_{1c} and 6.53 ppm for H_{2c}, respectively, suggesting that **3oo** is converted to **3co** whereas dually ring-closed isomer **3cc** is unattained (Scheme 3). As shown in Scheme 3 and Figure 2b, the methyl signals of **3oo** occur at 1.96 (methyl *a*) and 1.95 (methyl *b*) ppm. Upon being irradiated at 365 nm, while signals *a* and *b* are progressively reduced in intensity, two new signals at 2.17 (methyl *a*′) and 2.15 (methyl *b*′) and another two new signals at 1.98 (methyl *d*′) and 1.94 (methyl *c*′) ppm with slight shifts relative to signals *a* (1.96 ppm) and *b* (1.95 ppm) are progressively generated due to **3oo**→**3co** conversion. When the CD_2Cl_2 solution is sufficiently irradiated at 365 nm to the PSS, four methyl signals with similar peak intensity are exhibited at 2.17 (methyl a′), 2.15 (methyl b′), 1.98 (methyl d′) and 1.94 (methyl c′), respectively, ascribable to the four CH_3 groups of singly ring-closed product **3co**. Instead, the methyl signals due to dually ring-closed form **3cc** are unobserved, implying that **3co**→**3cc** conversion is indeed unattained.

Upon irradiation of **1oo** with UV light at 365 nm, while the ^{19}F NMR (Figure 3a) singlet at −132.2 ppm and two singlets

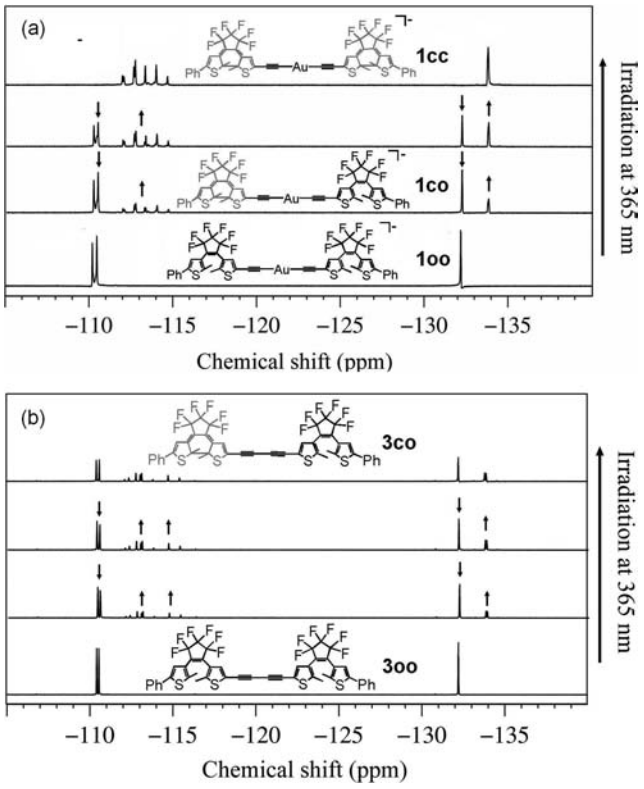

Figure 3. ^{19}F NMR spectral changes of **1oo** (a) and **3oo** (b) in CD_2Cl_2 upon irradiation at 365 nm, showing stepwise **1oo**→**1co**→**1cc** conversion, and **3oo**→**3co** conversion but without occurrence of **3co**→**3cc** conversion.

at −110.1 and −110.5 ppm are progressively reduced and disappeared finally, a singlet at −134.0 ppm and a set of multiplets at −112.0 to −114.8 ppm are increasingly generated, demonstrating further the occurrence of stepwise and dual photocyclization reactions **1oo**→**1co**→**1cc**. In contrast, when **3oo** (Figure 3b) is irradiated at 365 nm, a new doublet at −134.0 ppm and a set of multiplets at −112.0 to −115.5 ppm occur progressively. Meanwhile, the singlet at −132.2 ppm and two singlets at −110.3 and −110.5 ppm are gradually attenuated, but they do not vanish completely at the PSS, suggesting further the conversion of **3oo** to **3co**, but not to dually ring-closed form **3cc**.

Four-State and Four-Color Photochromism for 2ooo. Photochromic reactions and color changes for dinuclear gold(I) complex **2ooo** in CH_2Cl_2 solution and PMMA film are depicted in Scheme 4. Upon irradiation at 365 nm, colorless **2ooo** becomes sky-blue due to the selective photocyclization reaction of L2o, giving stepwise ring-closed product **2coc**. When **2coc** is further irradiated with UV light at 254 nm, the sky-blue is converted to deep purple−blue at the PSS because of further photocyclization reaction of L1o to give fully ring-closed isomer **2ccc**. If the deep purple−blue **2ccc** is irradiated with visible light at 672 nm, it changes into purple−red due to selective photocycloreversion reaction for L2c to produce **2oco**. Upon further irradiation of **2oco** with the light at >460 nm, the purple−red reverts to colorless due to the conversion of **2oco** into fully ring-open form **2ooo**. Thus, four ring-open/closed isomers with distinctly different colors have been attained upon irradiation with appropriate wavelengths of light through selective and stepwise photocyclization/cycloreversion of the coordinated DTE ligands L1 and L2.

In contrast with **2ooo**, stepwise and multiple photocyclization reactions could not be achieved for the corresponding model organic compound **4ooo** (Scheme 5) containing the same DTE units as revealed from UV−vis (Figure 4) and ^{1}H NMR (Figure 5) spectral studies. Upon irradiation of **4ooo** at 365 nm to the PSS, two new bands centered at 396 and 610 nm (Figure 4a) are increasingly enhanced with the attenuation of the band centered at 280 nm due to **4ooo**→**4coc** conversion. When **4coc** is further irradiated with UV light at 254 nm, however, distinct UV−vis spectral change (Figure 4b) is unobserved, indicating that further photocyclization reaction for the central nonfluorinated DTE unit (Scheme 5) does not occur so that fully ring-closed isomer **4ccc** is unattained. Upon irradiation of **4ooo** in a CD_2Cl_2 solution with UV light at 365 nm, while the ^{1}H NMR (Figure 5) spectral signals at 7.26 ppm for H_{1o} and 7.23 ppm for H_{2o} decrease progressively and disappear finally, the proton signals at 6.68 ppm for H_{1c} and 6.33 ppm for H_{2c} are observed due to **4ooo**→**4coc** conversion. Meanwhile, the signal at 6.96 ppm for H_{3o}/H_{4o} is a little low-field shifted to 7.03 ppm (H_{3o}'/H_{4o}'). Further irradiation of the solution with UV at 256 nm does not results in new signals for H_{3c}/H_{4c} as depicted in Figure 5, demonstrating that partially ring-closed form **4coc** is only generated whereas fully ring-closed isomer **4ccc** is inaccessible (Scheme 5).

The UV−vis absorption spectra of four ring-open/closed isomers **2ooo**/**2coc**/**2ccc**/**2oco** in CH_2Cl_2 solutions are presented in Figure 6. Intense absorption bands of fully ring-open form **2ooo** occur with the maxima at ca. 230 and 300 nm, ascribed to intraligand transitions of the thienyl moieties of L1o and L2o, respectively. For **2coc** with selective ring-closing at L2c, the low-energy absorption band centered at 600 nm is observed, which is obviously red-shifted compared with that in free ligand L2c (584 nm). Likewise, the low-energy band of **2oco** with selective ring-closing at L1c is distinctly red-shifted to 520 nm relative to that in free ligand L1c (510 nm). It is likely that the coordination of L1c and L2c to gold(I) ion results in an enhanced π-system and thus a distinct red-shift of the ^{1}IL states associated with spin−orbital coupling due to the heavy-atom effect of the gold(I) ion. It is known that the enhancement of π-system usually lowers HOMO−HOMO gap

dx.doi.org/10.1021/ic202265u | *Inorg. Chem.* 2012, 51, 1933−1942

Scheme 4. Photochromic Reactions and Color Conversions of 2ooo in CH_2Cl_2 Solution and PMMA Film (25%)

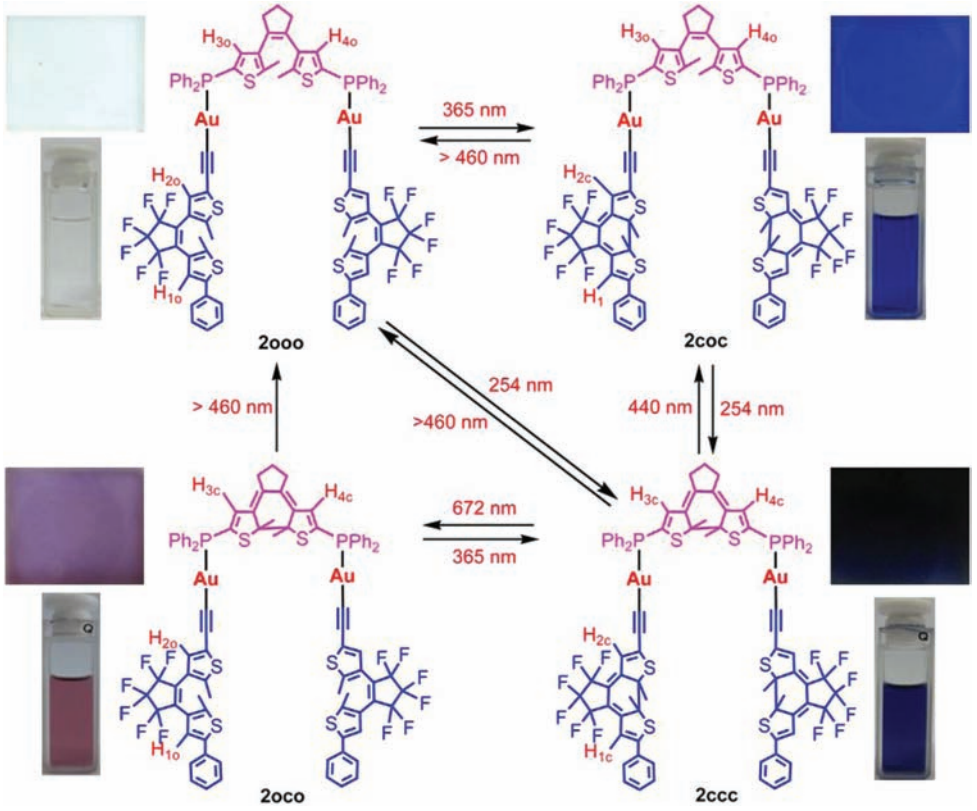

Scheme 5. Photochromic Reactions for 4ooo

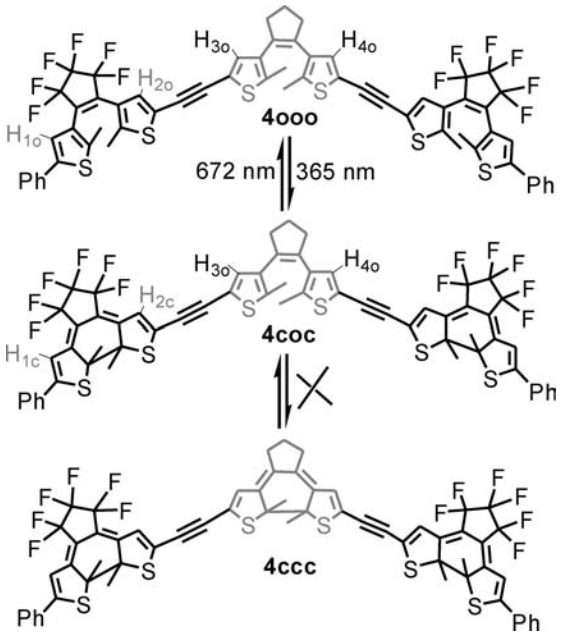

and thus a red-shift of the absorption.[8,9] The UV−vis absorption spectrum of fully ring-closed isomer **2ccc** is composed of the absorption components from both gold(I)-coordinated L1c and L2c. The broad low-energy absorption of **2ccc** (Figure S3) with the maximum at 563 nm tailing to 800 nm is somewhat blue-shifted compared with that of **2coc**.

DFT computational studies have been carried out to elucidate the UV−vis transition character of the four ring-open/closed isomers **2ooo**/**2coc**/**2ccc**/**2oco**. The low-energy absorptions (>300 nm) of fully ring-open isomer **2ooo** (Table 1) result mainly from intraligand transitions of L2o mixed with some L2o→L1o LLCT (ligand-to-ligand charge transfer) character. Thus, this makes it feasible for selective photocyclization reaction at L2o without affecting L1o upon irradiation at 365 nm, so that ring-closed form **2coc** is experimentally attainable. For selectively ring-closed isomers **2oco** (Table S4) or **2coc** (Table S6), the calculated low-energy absorption band centered at 522 nm for **2oco** or ca. 616 nm for **2coc** originates predominantly from ring-closed ligand L1c or L2c, respectively. The broad low-energy absorption (>500 nm) of fully ring-closed isomer **2ccc** (Table 2) is contributed by both ring-closed L1c and L2c. Because the low-energy absorption profile at >650 nm (Figure 6) is dominated by L2c with inappreciable contribution from L1c, it is experimentally feasible to attain **2oco** through selective cycloreversion reaction of L2c upon irradiation of fully ring-closed isomer **2ccc** at 672 nm. The calculated HOMO−LUMO gap follows **2ooo** (4.32 eV) > **2oco** (3.06 eV) > **2coc** (2.59 eV) ≈ **2ccc** (2.57 eV), agreeing well with the measured low-energy absorption bands with **2ooo** (301, 336sh nm) < **2oco** (520 nm) < **2coc** (600 nm) ≈ **2ccc** (563, 610 nm).

Photochemical quantum yields and conversion percentages at PSS are summarized in Table 3 for photochromic reactions of **2ooo**. As depicted in Figure 7a, when a CH_2Cl_2 solution of **2ooo** is irradiated at 365 nm, three new absorption bands centered at ca. 316, 383, and 600 nm occur due to formation of **2coc** with selective photocyclization reaction at L2o. These new bands are progressively increased in intensity before it reaches PSS. The photocyclization quantum yield $\Phi_{2ooo\rightarrow 2coc}$ is estimated as 0.24 (Table 3). Upon further irradiation of a CH_2Cl_2 solution of **2coc** with UV light at 254 nm as shown in

dx.doi.org/10.1021/ic202265u | Inorg. Chem. 2012, 51, 1933−1942

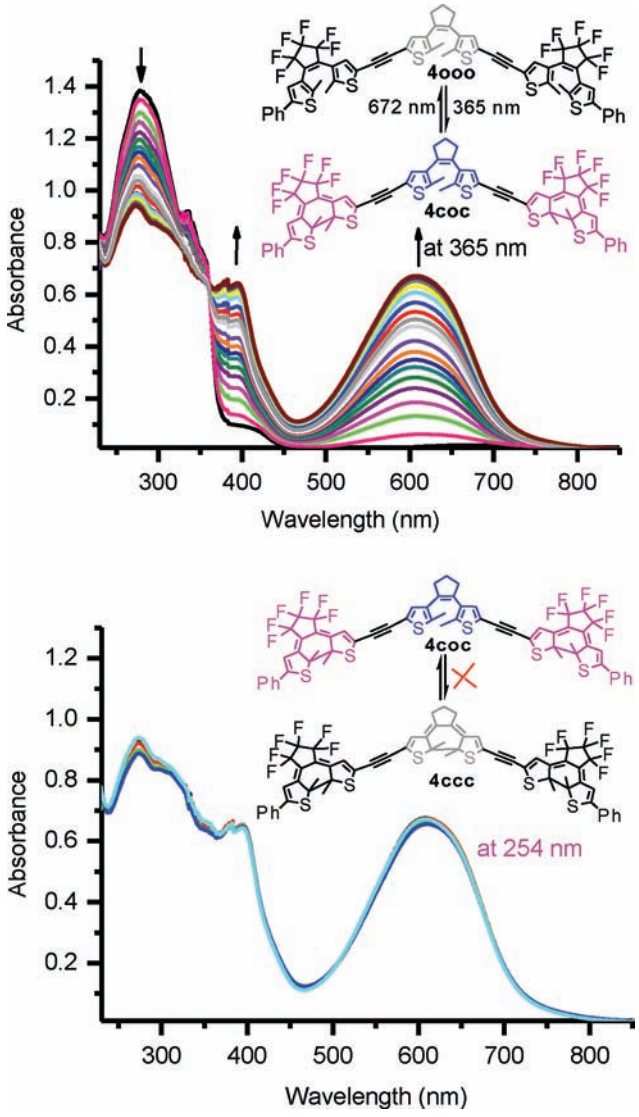

Figure 4. (a)UV−vis absorption spectral changes of **4ooo** in dichloromethane upon irradiation at 365 nm, showing **4ooo→4coc** conversion. (b) UV−vis absorption spectral changes of **4coc** in dichloromethane upon irradiation at 254 nm, in which distinct **4coc→4ccc** conversion was unobserved.

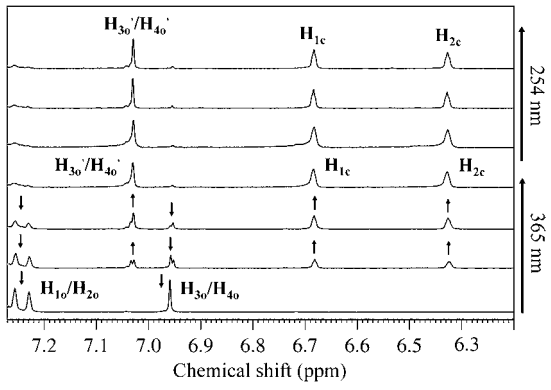

Figure 5. ^{1}H NMR spectral changes of **4ooo** in CD_2Cl_2 upon irradiation at 365 nm, showing **4ooo→4coc** conversion but further irradiation at 254 without occurrence of **4coc→4ccc** conversion.

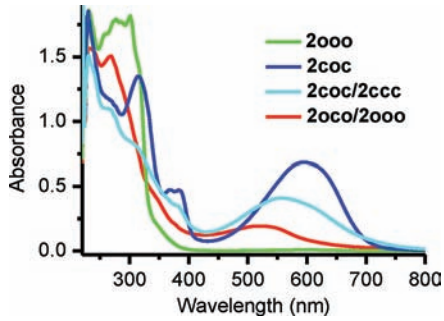

Figure 6. UV−vis absorption spectra of **2** in four ring-open/closed isomers measured in CH_2Cl_2 solutions at 298 K.

Figure 7b, while the absorptions at 231, 316, and 383 nm are reduced in intensity, the maximum at 600 nm is blue-shifted to 558 nm at the PSS due to the photocyclization reaction of L1o to give fully ring-closed isomer **2ccc** ($\Phi_{2coc\rightarrow2ccc}$ = 0.004). It is noteworthy that **2coc→2ccc** conversion is much slower than that of **2ooo→2coc** because the photocyclization reaction of L1o (53% for free L1o) is much less sensitive and effective than that of L2o (>95% for free L2o). Another possible factor to lower the conversion percentage of **2coc→2ccc** arises from intramolecular energy transfer in **2coc** from ring-open L1o to ring-closed L2c, in which the reactive excited state of L1o is partially quenched by the lower-lying excited state of the closed ring form of L2c in **2coc**. When the solution at the PSS is irradiated at 672 nm, the band at 558 nm is gradually attenuated whereas an absorption with maximum at 520 nm is observed (Figure S4), indicating that **2ccc** is converted to **2oco** due to the selective cycloreversion reaction at L2c with the deep purple−blue tuning into purple−red (Scheme 4). The **2oco→2ooo** transformation is readily attainable through the cycloreversion reaction of L1c upon irradiation at >460 nm (Figure S5) although the reverse photocyclization process **2ooo→2oco** is directly unattainable. Noticeably, the conversion processes **2ooo** ⇄**2coc** ⇄**2ccc** ⇄**2oco** are totally reversible and reproducible through stepwise and selective photocyclizition/cycloreversion reactions upon irradiation with suitable wavelengths of light as shown in Scheme 4. Alternatively, the **2ooo** ⇄**2ccc** conversion between fully ring-open form **2ooo** and fully ring-closed isomer **2ccc** can be directly attained through photocyclizition/cycloreversion reactions upon irradiation at 254 nm or >460 nm in the reverse process.

The photochromic cyclization/cycloreversion reactions (**2ooo** ⇄**2coc** ⇄**2ccc** ⇄**2oco**) have been monitored through ^{1}H NMR spectral changes in $CDCl_3$ (Figure 8, top). When the solution of **2ooo** is irradiated under UV light at 365 nm, the thienyl protons H_{1o} (7.24 ppm) and H_{2o} (7.17 ppm) of L2o decrease gradually and finally disappear. Meanwhile, two new signals at 6.64 (H_{1c}) and 6.33 (H_{2c}) ppm are generated because of the selective photocyclization reaction of L2o to L2c (Figure S8). Furthermore, the proton signals of H_{3o} and H_{4o} for L1o (Scheme 4) are a little upfield shifted to 7.15 ppm during **2ooo** ⇄**2coc** conversion. When the $CDCl_3$ solution of **2coc** is further irradiated at 254 nm, while the proton signals of H_{3o} and H_{4o} at 7.18 to 7.15 ppm decrease (Figure S9), two new peaks appear at 6.56 (H_{3c}) and 6.58 (H_{4c}) ppm due to photocyclization reaction of L1o so as to give fully ring-closed isomer **2ccc**. At the PSS, the signal intensity ratio of H_{3o}/H_{3c} or H_{4o}/H_{4c} is ca. 7: 3 (Figure S9). This implies that the

dx.doi.org/10.1021/ic202265u | Inorg. Chem. 2012, 51, 1933−1942

Table 1. Absorption Transitions and Singlet Excited States for 2ooo in Dichloromethane, Calculated by TD-DFT Method

	transition	contrib (%)	*E*, nm (eV)	O.S.	assignment	exp (nm)
S1	HOMO→LUMO+1	58	348 (3.56)	0.0784	^{1}IL (L2o)	336, 318
	HOMO-1→LUMO	42			^{1}IL (L2o)	
S6	HOMO-1→LUMO+3	26	307 (4.04)	1.6311	^{1}LLCT (L2o→L1o)/^{1}IL(L2o)	301
	HOMO-1→LUMO+2	21			^{1}LLCT (L2o→L1o)	
	HOMO→LUMO+3	20			^{1}LLCT(L2o→L1o) /^{1}IL(L2o)	
	HOMO→LUMO+2	13			^{1}LLCT (L2o→L1o)	
S15	HOMO-1→LUMO+6	27	288 (4.31)	0.6928	^{1}IL(L2o)/^{1}LLCT(L2o→L2o)	278
	HOMO-1→LUMO+5	26			^{1}IL(L2o)/^{1}LLCT(L2o→L2o)	
	HOMO→LUMO+5	21			^{1}IL(L2o)/^{1}LLCT(L2o→L2o)	
	HOMO→LUMO+6	14			^{1}IL(L2o)/^{1}LLCT(L2o→L2o)	

Table 2. Absorption Transitions and Singlet Excited States for 2ccc in Dichloromethane, Calculated by TD-DFT Method

	transition	contrib (%)	*E*, nm (eV)	O.S.	assignment	exp (nm)
S1	HOMO→LUMO	85	625 (1.98)	0.3218	^{1}IL (L2c)	610
S2	HOMO-1→LUMO+1	85	617 (2.01)	0.9073	^{1}IL (L2c)	563
S5	HOMO-2→LUMO+2	71	524 (2.37)	0.2538	^{1}IL (L1c)	513
	HOMO-2→LUMO	26			^{1}LLCT (L1c→L2c)	
S14	HOMO→LUMO+2	36	372 (3.33)	0.2945	^{1}LLCT (L2c→L1c)	385
	HOMO-2→LUMO	35			^{1}LLCT (L1c→L2c)	
	HOMO-3→LUMO	19			^{1}LLCT [L2c(right)→L2c(left)]	
S28	HOMO→LUMO+3	61	310 (3.99)	0.2072	^{1}LLCT/^{1}IL	312

Table 3. Photochemical Quantum Yields and Conversion Percentage at Photostationary State (PSS) for Photochromic Reactions of 2ooo

	photochemical quantum yield Φ^a		
	$\Phi_{o\text{-}c}$	$\Phi_{c\text{-}o}$	conversion at PSS (%)^b
2ooo	0.24^c (→**2coc**)		>95% (→**2coc**)
2coc	0.004^d (→**2ccc**)	0.006^e (→**2ooo**)	30% (→**2ccc**)
2ccc		0.0072^f (→**2oco**)	
		0.0005^g (→**2coc**)	
2oco	0.25^b (→**2ccc**)	0.002^e (→**2ooo**)	>95% (→**2ccc**)

^{a}Data obtained with an uncentainty of ±10%. ^{b}Conversion percentages measured by NMR spectroscopy. ^{c}Data obtained by irradiation with 365 nm light. ^{d}Data obtained by irradiation with 254 nm light. ^{e}Data obtained by irradiation with >460 nm light. ^{f}Measured by irradiation with 672 nm light. ^{g}Measured by irradiation with 440 nm light.

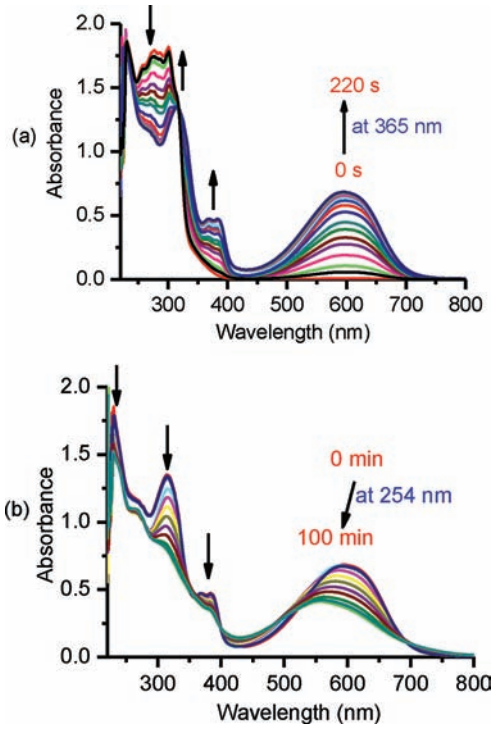

Figure 7. (a) UV−vis Absorption spectral changes of complex **2ooo** (2×10^{-5} M) in CH_2Cl_2 solution upon irradiation at 365 nm. (b) Absorption spectral changes of **2coc** (2×10^{-5} M) in CH_2Cl_2 solution upon irradiation at 254 nm to the PSS.

percentages of **2coc** and **2ccc** are 70% and 30%, respectively. Upon irradiation of the solution at the PPS (70% **2coc** and 30% **2ccc**) with visible light at 672 nm, while the signals at 6.64 (H_{1c}) and 6.33 (H_{2c}) ppm are gradually attenuated and finally disappeared (Figure S10), the corresponding proton peaks due to H_{1o} (7.24 ppm) and H_{2o} (7.17 ppm) occur at a lower field. This suggests selective cycloreversion reaction occurs at L2c, resulting in the conversion process **2ccc**/**2coc**→**2oco**/**2ooo**. If the solution at this stage (**2ooo**/**2oco**) is further irradiated with the light at >460 nm, the proton signals at 6.56 (H_{3c}) and 6.58 (H_{4c}) are reduced and finally disappear, revealing that **2oco** is entirely converted to fully ring-open isomer **2ooo** through cycloreversion reaction at L1c (Figure S11).

The photochromic conversions have been also supported by ^{31}P NMR spectroscopy (Figure 8, lower or Figure S14). When a $CDCl_3$ solution of **2ooo** is irradiated at 365 nm, while the P signal at 29.0 ppm decreases gradually and vanishes finally, a new P signal is observed at 28.6 ppm due to the selective photocyclization reaction of L2o to give **2coc**. Upon further irradiation of the solution (**2coc**) with UV light at 254 nm, the P signal at 28.6 ppm decreases gradually whereas a new peak occurs at 35.0 ppm due to **2coc**→**2ccc** transformation resulting from photocyclization reaction of L1o to L1c. The P signal integral intensity ratio between **2coc** (28.6 ppm) and **2ccc** (35.0 ppm) is 7:3 at the PSS, suggesting 70% of **2coc** and 30%

dx.doi.org/10.1021/ic202265u | *Inorg. Chem.* 2012, 51, 1933−1942

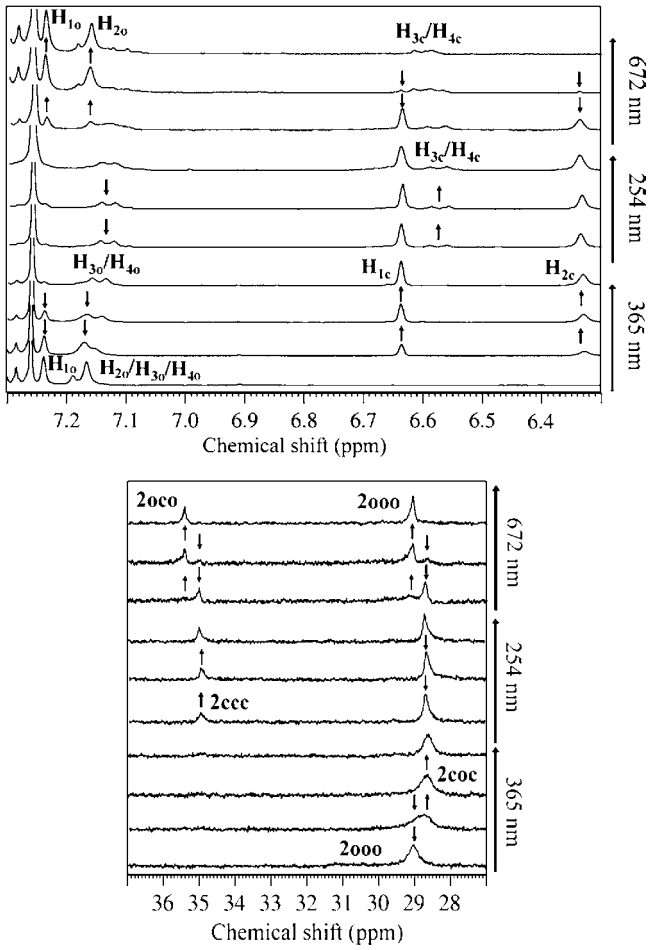

Figure 8. ^{1}H (top) and ^{31}P NMR (lower) spectral changes of **2ooo** in $CDCl_3$ upon irradiation at 365 nm showing **2ooo**→**2coc** conversion, further irradiation at 254 nm to the PPS showing **2coc**→**2ccc** conversion, and then irradiation at 672 nm showing **2ccc**/**2coc**→**2oco**/**2ooo** conversion.

of **2ccc**, the same as that from the ^{1}H NMR spectral studies. When the solution of **2coc**/**2ccc** is further irradiated at 672 nm, with the gradual decay and final disappearance of the P signals at 28.6 ppm for **2coc** and 35.0 ppm for **2ccc**, those at 29.0 ppm for **2ooo** and at 35.5 ppm for **2oco** are generated and enhanced progressively, suggesting that **2coc** and **2ccc** have been converted to **2ooo** and **2oco**, respectively. Upon further irradiation of the solution (**2oco**/**2ooo**) at >460 nm (Figure S16), the signal at 35.5 ppm for **2oco** is gradually attenuated and finally disappears whereas the signal at 29.0 ppm for **2ooo** is progressively increased because of **2oco**→**2ooo** conversion through the cycloreversion reaction of L1c to L1o.

Although the ^{19}F NMR spectra are insensitive to the photochromic reactions **2coc**⇄**2ccc** or **2oco**→**2ooo** due to photocyclization/cycloreversion reaction of ligand L1o/L1c without containing F atoms, significant ^{19}F NMR spectral changes are indeed observed for the conversion **2ooo** ⇄**2coc** or **2ccc**⇄**2oco** that is involved in photochromic reaction on hexafluoro ligand L2o/L2c. The solution of **2ooo** (Figure S17) exhibits one signal at −131.8 ppm and two signals at −110.0 and −110.2 ppm with the intensity ratio of 1:1:1. Upon irradiation at 365 nm, while the signal at −131.8 ppm is gradually reduced, a low-field shifted signal is observed at −133.5 ppm due to the photocyclization reaction of L2o to produce selectively ring-closed isomer **2coc**. Meanwhile, the two signals at −110.0 and −110.2 ppm are progressively decreased and finally disappeared (Figure S17), whereas four set of doublets are detected at −111.5 to −114.2 ppm. Similarly, the reverse ^{19}F NMR spectral changes (Figure S18) are observed when **2ccc** is gradually converted to **2oco** due to the cycloreversion reaction of L2c to L2o upon irradiation at 672 nm.

Although four ring-open/closed isomers **2ooo**/**2coc**/**2ccc**/**2oco** have been successfully achieved for dinuclear gold(I) complex **2** upon irradiation with appropriate wavelengths of light, it is noticeable that stepwise or selective photochromic reactions do not occur at the two L2 ligands. From both NMR and UV−vis spectral studies, it is found that the two L2 are simultaneously ring-opening or -closed to afford **2ooo** (**2oco**) or **2coc** (**2ccc**), respectively, whereas states **2ooc**/**2coo** or **2occ**/**2cco** are never observed through stepwise or selective photocyclization/cycloreversion reactions at the two L2. It appears that a long separation (Au-L1-Au) between the two L2 is unfavorable for stepwise or selective photochromic reaction.

■ CONCLUSIONS

A mononuclear gold(I) complex with two identical DTE-acetylides and a dinuclear gold(I) complex with both DTE-acetylide and DTE-diphosphine are elaborately designed and prepared, which exhibit multistep and multiple photochromic properties upon irradiation with appropriate wavelengths of light. For the corresponding model organic compounds containing the same DTE units, however, fully ring-closed isomers through multiple photocyclization reactions are unattainable, demonstrating that gold(I) coordination plays a key role in achieving stepwise and multiple photochromic switch. It appears that the coordinated gold(I) atom acts as an effective "barrier" to prohibit intramolecular energy transfer between multi-DTE moieties. Therefore, incorporating multi-DTE moieties into a proper metal coordinated system affords a feasible strategy to attain multiple and multistep photochromic switch in a metal complex with multi-DTE components.

■ EXPERIMENTAL SECTION

General Procedures and Materials. All the synthetic operations were carried out by using Schlenk techniques and vacuum-line systems under a dry argon atmosphere unless otherwise specified. Solvents were distilled under nitrogen from sodium and benzophenone (THF) or calcium hydride. L1o,[29] L2o,[21] and $[N(PPh_3)_2][Au(acac)_2]$[30] were prepared according to the literature procedures. Other chemicals were commercially available.

*$[N(PPh_3)_2][Au(L2o)_2]$ (**1oo**).* A mixture of $[N(PPh_3)_2][Au(acac)_2]$ (46.6 mg, 0.05 mmol) and L2o (70 mg, 0.15 mmol) was stirred in acetone (15 mL) at room temperature for 2 h. The reaction was monitored by TLC. Upon completion, the solution was concentrated under reduced pressure to 2 mL, to which *n*-hexane was then added to precipitate the product as a white solid. Yield: 55% (45 mg). Anal. Calcd for $C_{82}H_{56}AuF_{12}NP_2S_4$: C, 58.96; H, 3.38; N, 0.84. Found: C, 58.62; H, 3.25; N, 0.93. ESI-MS: *m*/*z* (%) 1131 (100) $[Au(L2o)_2]^-$, 538.7 (100) $[PPN]^+$. ^{1}H NMR (CD_2Cl_2, ppm): δ 7.66−7.62 (m, 6H), 7.52 (d, J = 7.44 Hz, 4H), 7.47−7.42 (m, 24H), 7.36 (t, J = 7.60 Hz, 4H), 7.27 (t, J = 7.36 Hz, 2H), 7.25 (s, 2H), 6.94 (s, 2H), 1.93 (s, 6H), 1.81 (s, 6H). ^{31}P NMR (CD_2Cl_2, ppm): δ 21.03. IR (KBr, cm^{-1}): 2092 (C≡C).

$Au_2(L1o)_2Cl_2$. A solution of Au(tht)Cl (64 mg, 0.2 mmol) in CH_2Cl_2 (15 mL) was added dropwise with a solution of L1o (62.8 mg, 0.1 mmol) in CH_2Cl_2 (5 mL) at room temperature. Upon stirring for 2 h, the solvent was removed under reduced pressure and the resulting solid was recrystallized from dichloromethane/*n*-hexane to give a

dx.doi.org/10.1021/ic202265u | Inorg. Chem. 2012, 51, 1933−1942

white solid. Yield: 92% (101 mg). Anal. Calcd for $C_{39}H_{34}Au_2Cl_2P_2S_2$: C, 42.83; H, 3.13. Found: C, 43.11; H, 3.25. MS (ESI-MS): m/z (%) 1093 (100) $[M + 1]^+$. ^1H NMR ($CDCl_3$, ppm) δ 7.52−7.42 (m, 20H), 7.11 (d, J = 9.52 Hz, 2H), 2.75 (t, J = 7.40 Hz, 4H), 2.09−2.01 (m, 2H), 2.03 (s, 6H). ^{31}P NMR ($CDCl_3$, ppm): δ 18.90.

2ooo. Complex $Au_2(L1o)_2Cl_2$ (54.6 mg, 0.05 mmol) and sodium methoxide (6.6 mg, 0.12 mmol) were added to a dry THF-MeOH (20 mL, v/v = 1:1) solution of L2o (51.2 mg, 0.11 mmol) with stirring at room temperature. The reaction was monitored by TLC. When the reaction finished, the solvents were removed under reduced pressure. The residue was then dissolved in 10 mL of CH_2Cl_2. The solution was filtered through Celite. Layering *n*-hexane onto the concentrated CH_2Cl_2 solution gave complex **2ooo** as a white solid. Yield: 48% (47 mg). Anal. Calcd for $C_{85}H_{60}Au_2F_{12}P_2S_6$: C, 52.15; H, 3.09. Found: C, 52.35; H, 3.15. ^1H NMR ($CDCl_3$, ppm) δ 7.54−7.47 (m, 16H), 7.43−7.35 (m, 12H), 7.30−7.28 (m, 2H), 7.24 (s, 2H), 7.19−7.17 (m, 4H), 2.75 (t, J = 7.32 Hz, 4H), 2.07−2.03 (m, 2H), 2.00 (s, 6H), 1.92 (s, 6H), 1.87 (s, 6H). ESI-MS: m/z (%) = 1489 (100) $[Au_2(L1o)(L2o)]^+$. ^{31}P NMR ($CDCl_3$, ppm): δ 29.0. IR (KBr): 2106 cm^{-1} (w, C≡C).

3oo. A mixture of L2o (117 mg, 0.25 mmol), CuCl (4 mg), and piperidine (20 mg, 0.25 mmol) was added into toluene (10 mL). The mixture was heated with stirring at 60 °C for 5 h. The reaction was monitored by TLC. Upon completion, the solution was concentrated under reduced pressure. The product was purified by silica gel column chromatography using dichloromethane-petroleum ether (v/v = 1:4) as eluent. Yield: 77% (90 mg). ESI-MS: m/z (%) 935 (100) $[M + 1]^+$. ^1H NMR (CD_2Cl_2, ppm): δ 7.54−7.52 (m, 4H), 7.39−7.34 (m, 4H), 7.37 (s, 2H), 7.31−7.27 (m, 2H), 7.24 (s, 2H), 1.95 (s, 6H), 1.94 (s, 6H).

1,2-Bis(5-iodo-2-methylthiophen-3-yl)cyclopentene. To an anhydrous THF (12 mL) solution of 1,2-bis(5-chloro-2-methylthiophen-3-yl)cyclopentene (460 mg, 1.40 mmol) was added slowly *n*-BuLi (1.6 M in hexane, 1.87 mL, 3 mmol) using a syringe. After the reaction mixture was stirred for 30 min at room temperature, an anhydrous THF solution of iodine (2.2 g, 8.64 mmol) was slowly added. The reaction was monitored by TLC. Upon stirring for 5 h, the reaction was quenched by an aqueous solution of sodium thiosulfate. The aqueous layer was separated from the organic layer and extracted with diethyl ether which was dried with $MgSO_4$. The product was purified by silica gel column chromatography using petroleum ether as eluent. Yield: 78% (560 mg). ESI-MS: m/z (%) 513 (100) $[M + 1]^+$. ^1H NMR ($CDCl_3$, ppm): δ 6.89 (s, 2H), 2.73 (t, J = 7.6 Hz, 4H), 2.05−2.00 (m, 2H), 1.89 (s, 3H), 1.85 (s, 3H).

4ooo. 1,2-Bis(5-iodo-2-methylthiophen-3-yl)cyclopentene (51.2 mg, 0.1 mmol) was dissolved in diisopropylamine (15 mL) at room temperature. To the solution were added $Pd(PPh_3)_2Cl_2$ (17 mg, 0.01 mmol) and CuI (2 mg) with stirring for 15 min. Compound L2o (112 mg, 0.24 mmol) was then added and the reaction mixture was stirred for another 2 h at room temperature. The reaction was monitored by TLC. Upon completion, the solution was first filtered and the filtrate was then concentrated under reduced pressure. The product was purified by silica gel column chromatography using dichloromethane-petroleum ether (v/v = 1:2) as eluent. Yield: 70% (83 mg). ESI-MS: m/z (%) 1193 (100) $[M + 1]^+$. ^1H NMR (CD_2Cl_2, ppm): δ 7.55−7.52 (m, 4H), 7.37 (t, J = 7.5 Hz, 4H), 7.31−7.28 (m, 2H), 7.26 (s, 2H), 7.23 (s, 2H), 6.96 (s, 2H), 2.76 (t, J = 7.46 Hz, 3H), 2.12−2.08 (m, 3H), 1.96 (s, 6H), 1.95 (s, 6H), 1.93 (s, 6H).

Physical Measurements. ^1H, ^{19}F, and ^{31}P NMR spectra were performed on a Bruker Avance III (400 MHz) spectrometer with $SiMe_4$ as the internal reference and H_3PO_4 as the external reference. UV−vis absorption spectra were measured on a Perkin-Elmer Lambda 25 UV−vis spectrophotometer. Infrared spectra (IR) were recorded on a Magna 750 FT-IR spectrophotometer with KBr pellets. Elemental analyses (C, H, and N) were carried out on a Perkin-Elmer model 240 C elemental analyzer. Electrospray ionization mass spectrometry (ESI-MS) was recorded on a Finnigan DECAX-30000 LCQ mass spectrometer using dichloromethane-methanol as mobile phase. ZF5 UV lamp (254 and 365 nm) was used for UV light irradiation, and visible light irradiation (440, 672, or >460 nm) was carried out by using a LZG220 V500 W tungsten lamp with cutoff filters. The quantum yields were determined by comparing the reaction yields of the diarylethenes against 1,2-bis(2-methyl-5-phenyl-3-thienyl)perfluorocyclopentene.[31]

Theoretical Methodology. The ground state geometry of **2ooo**, **2coc**, **2oco**, or **2ccc** was optimized using Kohn−Sham DFT[32] with the gradient corrected correlation functional level PBE1PBE.[33] Based on the optimized ground state geometries, sixty singlet and six triplet excited states were obtained to determine the vertical excitation energies and the oscillator strengths for **2ooo**, **2coc**, **2oco**, or **2ccc** using the time-dependent DFT (TD-DFT) method at the same level mentioned above.[34,35] The conductor-like polarizable continuum model (PCM)[36] with dichloromethane as solvent was used to calculate in solution. It is a general technique to employ hydrogen to substitute phenyl in ab initio calculations to save computational resources. Häberlen and Rösch[37] have proved that PH_3 provides a satisfactory model of the full PMe_3 or PPh_3 for the structural properties of gold(I) complexes. In these calculations, the Hay−Wadt double-ξ with a Los Alamos relativistic effect basis set (LANL2DZ)[38] consisting of the effective core potentials (ECP) was employed for the Au atom and 6-31G* basis set was used for the remaining atoms. To precisely describe the molecular properties, one additional *f*-type polarization function was implemented for Au(I) atom (α = 0.2).[39] All the calculations were carried out by using the suite of Gaussian 03 program package.[40]

■ ASSOCIATED CONTENT

Ⓢ Supporting Information

Figures giving additional spectral properties, and tables and figures of DFT calculations. This material is available free of charge via the Internet at http://pubs.acs.org.

■ AUTHOR INFORMATION

Corresponding Author

*E-mail: czn@fjirsm.ac.cn.

■ ACKNOWLEDGMENTS

We thank financial support from the NSFC (20931006, U0934003, and 91122006), the 973 project (2007CB815304) from MSTC, and the NSF of Fujian Province (2011J01065).

■ REFERENCES

(1) (a) Kume, S.; Nishihara, H. *Dalton Trans.* **2008**, 3260. (b) Ko, C.-C.; Yam, V. W.-W. *J. Mater. Chem.* **2010**, *20*, 2063. (c) Bouas-Laurent, H.; Burr, H. *Pure Appl. Chem.* **2001**, *73*, 639.

(2) (a) Irie, M. *Chem. Rev.* **2000**, *100*, 1685. (b) Matsuda, K.; Irie, M. *J. Photochem. Photobiol. C* **2004**, *5*, 169.

(3) (a) Tian, H.; Yang, S. J. *Chem. Soc. Rev.* **2004**, *33*, 85. (b) Tian, H.; Wang, S. *Chem. Commun.* **2007**, 781. (c) Tian, H.; Feng, Y. *J. Mater. Chem.* **2008**, *18*, 1617.

(4) (a) Higashiguchi, K.; Matsuda, K.; Tanifuji, N.; Irie, M. *J. Am. Chem. Soc.* **2005**, *127*, 8922. (b) Higashiguchi, K.; Matsuda, K.; Irie, M. *Angew. Chem., Int. Ed.* **2003**, *42*, 3537. (c) Myles, A. J.; Wigglesworth, T. J.; Branda, N. R. *Adv. Mater.* **2003**, *15*, 745. (d) Liu, H.-H.; Chen, Y. *J. Mater. Chem.* **2011**, *21*, 1246.

(5) (a) Andreasson, J.; Straight, S. D.; Moore, T. A.; Moore, A. L.; Gust, D. *J. Am. Chem. Soc.* **2008**, *130*, 11122. (b) Andrasson, J.; Pischel, U.; Straight, S. D.; Moore, T. A.; Moore, A. L.; Gust, D. *J. Am. Chem. Soc.* **2011**, *133*, 11641. (c) Sakamoto, R.; Murata, M.; Kume, S.; Sampei, H.; Sugimoto, M.; Nishihara, H. *Chem. Commun.* **2005**, 1215. (d) Sakamoto, R.; Kume, S.; Sugimoto, M.; Nishihara, H. *Chem.—Eur. J.* **2009**, *15*, 1429.

(6) Roberts, M. N.; Carling, C. J.; Nagle, J. K.; Branda, N. R.; Wolf, M. O. *J. Am. Chem. Soc.* **2009**, *131*, 16644.

(7) Browne, W. R. *Coord. Chem. Rev.* **2008**, *252*, 2470.

(8) Guerchais, V.; Ordronneau, L.; Bozec, H. L. *Coord. Chem. Rev.* **2010**, *254*, 2533.

(9) Hasegawa, Y.; Nakagawa, T.; Kawai, T. *Coord. Chem. Rev.* **2010**, *254*, 2643.
(10) Akita, M. *Organometallics* **2011**, *30*, 43.
(11) (a) Yam, V. W. W.; Ko, C. C.; Zhu, N. Y. *J. Am. Chem. Soc.* **2004**, *126*, 12734. (b) Lee, P. H. M.; Ko, C. C.; Zhu, N. Y.; Yam, V. W. W. *J. Am. Chem. Soc.* **2007**, *129*, 6058.
(12) Green, K. A.; Cifuentes, M. P.; Corkery, T. C.; Samoc, M.; Humphrey, M. G. *Angew. Chem., Int. Ed.* **2009**, *48*, 7867.
(13) Muratsugu, S.; Kume, S.; Nishihara, H. *J. Am. Chem. Soc.* **2008**, *130*, 7204.
(14) Liu, Y.; Lagrost, C.; Costuas, K.; Tchouar, N.; Bozec, H. L.; Rigaut, S. *Chem. Commun.* **2008**, 6117.
(15) Tanaka, Y; Inagaki, A.; Akita, M. *Chem. Commun.* **2007**, 1169.
(16) Tanaka, Y.; Ishisaka, T.; Inagaki, A.; Koike, T.; Lapinte, C.; Akita, M. *Chem.—Eur. J.* **2010**, *16*, 4762.
(17) Morimoto, M.; Miyasaka, H.; Yamashita, M.; Irie, M. *J. Am. Chem. Soc.* **2009**, *131*, 9823.
(18) Zhong, Y.-W.; Vila, N.; Henderson, J. C.; Flores-Torres, S.; Abruna, H. D. *Inorg. Chem.* **2007**, *46*, 10470.
(19) (a) Jukes, R. T. F.; Adamo, V.; Hartl, F.; Belser, P.; De Cola, L. *Inorg. Chem.* **2004**, *43*, 2779. (b) Fraysse, S.; Coudret, C.; Launay, J.-P. *Eur. J. Inorg. Chem.* **2000**, 1581.
(20) Lin, Y.; Yuan, J.; Hu, M.; Cheng, J.; Yin, J.; Jin, S.; Liu, S. H. *Organometallics* **2009**, *28*, 6402.
(21) Roberts, M. N.; Nagle, J. K.; Finden, J. G.; Branda, N. R.; Wolf, M. O. *Inorg. Chem.* **2009**, *48*, 19.
(22) Zhong, Y.-W.; Vila, N.; Henderson, J. C.; Abruna, H. D. *Inorg. Chem.* **2009**, *48*, 7080.
(23) Luo, Q.; Chen, B.; Wang, M.; Tian, H. *Adv. Funct. Mater.* **2003**, *13*, 233.
(24) Luo, Q.; Cheng, S.; Tian, H. *Tetrahedron Lett.* **2004**, *45*, 7737.
(25) Yam, V. W.-W.; Lee, J. K.-W.; Ko, C.-C.; Zhu, N. *J. Am. Chem. Soc.* **2009**, *131*, 912.
(26) Wong, H.-L.; Tao, C.-H.; Zhu, N.; Yam, V. W.-W. *Inorg. Chem.* **2011**, *50*, 471.
(27) Kim, H. J.; Jang, J. H.; Choi, H.; Lee, T.; Ko, J.; Yoon, M.; Kim, H.-J. *Inorg. Chem.* **2008**, *47*, 2411.
(28) Jung, I.; Choi, H.; Kim, E.; Lee, C.-H.; Kang, S. O.; Ko, J. *Tetrahedron* **2005**, *61*, 12256.
(29) (a) Yin, J.; Lin, Y.; Cao, X. F.; Yu, G. A.; Tu, H.; Liu, S. H. *Dyes Pigments* **2009**, *81*, 152. (b) Lin, Y.; Yin, J.; Yuan, J.; Hu, M.; Li, Z.; Yu, G.-A.; Liu, S. H. *Organometallics* **2010**, *29*, 2808.
(30) Vicente, J.; Chicote, M. T. *Inorg. Synth.* **1998**, *32*, 172.
(31) Irie, M.; Lifka, T.; Kobatake, S.; Kato, N. *J. Am. Chem. Soc.* **2000**, *122*, 4871.
(32) Becke, A. D. *J. Chem. Phys.* **1993**, *98*, 5648.
(33) Perdew, J. P.; Burke, K.; Ernzerhof, M. *Phys. Rev. Lett.* **1997**, *78*, 1396.
(34) Casida, M. E.; Jamorski, C.; Casida, K. C.; Salahub, D. R. *J. Chem. Phys.* **1998**, *108*, 4439.
(35) Stratmann, R. E.; Scuseria, G. E.; Frisch, M. J. *J. Chem. Phys.* **1998**, *109*, 8218.
(36) (a) Cossi, M.; Scalmani, G.; Regar, N.; Barone, V. *J. Chem. Phys.* **2002**, *117*, 43. (b) Barone, V.; Cossi, M. *J. Chem. Phys.* **1997**, *107*, 3210.
(37) Häberlen, O. D.; Rösch, N. *J. Phys. Chem.* **1993**, *97*, 4970.
(38) (a) Wadt, W. R.; Hay, P. J. *J. Chem. Phys.* **1985**, *82*, 284. (b) Hay, P. J.; Wadt, W. R. *J. Chem. Phys.* **1985**, *82*, 299.
(39) (a) Pyykkő, P.; Runeberg, N.; Mendizabal, F. *Chem.—Eur. J.* **1997**, *3*, 1451. (b) Pyykkő, P.; Mendizabal, F. *Chem.—Eur. J.* **1997**, *3*, 1458. (c) Pyykko, P.; Mendizabal, F. *Inorg. Chem.* **1998**, *37*, 3018.
(40) Frisch, M. J.; Trucks, G. W.; Schlegel, H. B.; Scuseria, G. E.; Robb, M. A.; Cheeseman, J. R.; Montgomery, J. A., Jr.; Vreven, T.; Kudin, K. N.; Burant, J. C.; Millam, J. M.; Iyengar, S. S.; Tomasi, J.; Barone, V.; Mennucci, B.; Cossi, M.; Scalmani, G.; Rega, N.; Petersson, G. A.; Nakatsuji, H.; Hada, M.; Ehara, M.; Toyota, K.; Fukuda, R.; Hasegawa, J.; Ishida, M.; Nakajima, T.; Honda, Y.; Kitao, O.; Nakai, H.; Klene, M.; Li, X.; Knox, J. E.; Hratchian, H. P.; Cross, J. B.; Bakken, V.; Adamo, C.; Jaramillo, J.; Gomperts, R.; Stratmann, R. E.; Yazyev, O.; Austin, A. J.; Cammi, R.; Pomelli, C.; Ochterski, J. W.; Ayala, P. Y.; Morokuma, K.; Voth, G. A.; Salvador, P.; Dannenberg, J. J.; Zakrzewski, V. G.; Dapprich, S.; Daniels, A. D.; Strain, M. C.; Farkas, O.; Malick, D. K.; Rabuck, A. D.; Raghavachari, K.; Foresman, J. B.; Ortiz, J. V.; Cui, Q.; Baboul, A. G.; Clifford, S.; Cioslowski, J.; Stefanov, B. B.; Liu, G.; Liashenko, A.; Piskorz, P.; Komaromi, I.; Martin, R. L.; Fox, D. J.; Keith, T.; Al-Laham, M. A.; Peng, C. Y.; Nanayakkara, A.; Challacombe, M.; Gill, P. M. W.; Johnson, B.; Chen, W.; Wong, M. W.; Gonzalez, C.; Pople, J. A. *Gaussian 03, revision C.02*. Gaussian, Inc.: Wallingford, CT, 2004.